

Weak decays of B_s to D_s based on the helicity analysis

Sara Rahmani^{1,*}

¹*School of Physics and Electronics,
Hunan University, Changsha 410082, China*

Abstract

Employing dipole and exponential hadronic transition form factors and helicity analysis combined with the Lattice QCD input, we present a detailed study of the decays $B_s \rightarrow D_s^{(*)} \ell \nu_\ell$. $B_s \rightarrow D_s + P(V)$, where $P = \pi^+, K^+, D_s^+$ and $V = \rho^+, K^{*+}, D_s^{*+}$, are also investigated and their branching fractions are examined. At the large recoil point, we calculate $f_{+,0}^{B_s \rightarrow D_s}(0) = 0.67 \pm 0.01$ for both parameterizations. Then we evaluate the branching fractions $BR(B_s \rightarrow D_s \ell \nu)$ and $BR(B_s \rightarrow D_s \ell \nu)$, which leads to $R(D_s) = 0.298 \pm 0.123$. The ratios $\frac{\Gamma(B_s^0 \rightarrow D_s^- \mu^+ \nu_\mu)}{\Gamma(B_s^0 \rightarrow D_s^{*-} \mu^+ \nu_\mu)}$ are found to be 0.4415 ± 0.1860 and 0.4406 ± 0.1854 , which are in good agreement of recent LHCb collaboration measurement. We also calculate the physical observables, $A_{FB}^\ell, P_L^\ell, P_T^\ell, C_F^\ell, F_L^\ell$.

arXiv:2409.02460v2 [hep-ph] 13 Mar 2025

*Electronic address: s.rahmani120@gmail.com

I. INTRODUCTION

The weak decay processes of B_s have been one of the most fascinating subjects for testing the Standard Model (SM) and provide a good source of knowledge in physics beyond SM, considering that the lepton flavor universality can be explored in these types of decay processes [1, 2]. All electroweak gauge bosons, Z^0, γ, W^\pm have equivalent interactions to the three leptonic generations in lepton flavor universality and the only divergence comes from the mass distinctions of e, μ, τ .

The experimental predictions of some physical observables such as ratios $R_D, R_{D^*}, R_{J/\psi}$ and longitudinal polarization of the final vector meson D^* , F_L^τ and the longitudinal polarization of the lepton τ , P_L^τ in B decays mediated by the quark level $b \rightarrow c\ell\bar{\nu}_\ell$ have disparities from SM predictions. In 2020, LHCb collaboration reported the first measurements of $B_s^0 \rightarrow D_s^{*-}\mu^+\nu_\mu$ to be $BR(B_s^0 \rightarrow D_s^-\mu^+\nu_\mu) = (2.49 \pm 0.12 \pm 0.14 \pm 0.16)$ and $BR(B_s^0 \rightarrow D_s^{*-}\mu^+\nu_\mu) = (5.38 \pm 0.25 \pm 0.46 \pm 0.30)$ [3], where the first, second and third uncertainties refer to statistical, systematic, and from the external inputs respectively. They also determined the ratio of $BR(B_s^0 \rightarrow D_s^-\mu^+\nu_\mu)/BR(B_s^0 \rightarrow D_s^{*-}\mu^+\nu_\mu)$ to be $0.464 \pm 0.013 \pm 0.043$. Belle Collaboration reported the ratios of branching fractions $BR(\bar{B} \rightarrow D^{(*)}\tau^-\bar{\nu}_\tau)/BR(\bar{B} \rightarrow D^{(*)}\ell^-\bar{\nu}_\ell)$ as $R(D) = 0.307 \pm 0.037 \pm 0.016$ and $R(D^*) = 0.283 \pm 0.018 \pm 0.014$ in B decays measurements [4]. The SM predictions are 0.298 ± 0.004 for $R(D)$ and 0.254 ± 0.005 in case of $R(D^*)$ in Ref. [5]. Heavy Flavor Averaging Group Collaboration also reported the branching fractions of two body decays of B_s^0 as follows: $BR(B_s^0 \rightarrow D_s^-\pi^+) = (2.85 \pm 0.18) \times 10^{-3}$, $BR(B_s^0 \rightarrow D_s^-K^+) = (0.213 \pm 0.014) \times 10^{-3}$, and $BR(B_s^0 \rightarrow D_s^-\rho^+) = (7.7_{-1.8}^{+1.9}) \times 10^{-3}$ [5]. The transition form factors of $B_s \rightarrow D_s$ have been studied by using the light-cone sum rules as well as heavy quark effective field theory and discussed the branching fractions of semileptonic $BR(B_s \rightarrow D_s\ell\nu)$, $\ell = e, \mu, \tau$ [6]. Hu *et al.* studied semileptonic B decays using perturbative QCD factorization with the Lattice QCD input [7]. Semileptonic and noneptonic decays of B_s have been investigated in the nonrelativistic constituent quark models [8]. The bottom transitions to the charm ones are discussed within Isgur-Wise functions in Refs. [9–12]. Zhou *et al.* evaluated the ratios of $R(D_s^{(*)}), R(D^{(*)})$ based on improved instantaneous Bethe–Salpeter method and relativistic corrections of the form factors [13]. Cui *et al.* computed the next-to-leading-order QCD computations of the $B_s \rightarrow D_s^{(*)}\ell\nu$ [14]. Angular analysis of $b \rightarrow c$ decays have been performed and several observables in SM and beyond have been studied [15, 16]. Lattice QCD determinations of the decays $B_s \rightarrow D_s\ell\nu$ and $B_s \rightarrow D_s^*\ell\nu$ have been done by HPQCD Collaborations in Ref. [17] and Ref. [18] respectively. We will use their data to perform fits in our model.

Motivated by the tensions between experimental measurements and theoretical SM predictions, we aim to study modes involving $B_s \rightarrow D_s^{(*)}$ in both semileptonic and noneptonic sectors. In the next section, we will present our formalism including helicity amplitudes II A, twofold angular distribution II B, physical observables II C, the formulations of two body decays $B_s \rightarrow D_s P$ and $B_s \rightarrow D_s V$ II D, and form factors II E. In section III, we will give a detailed numerical analysis and discuss the results of section II. Finally, Concluding remarks are provided in section IV.

II. FORMALISM

A. Helicity amplitudes

The effective Fermi Lagrangian for the semileptonic b to c induced transitions reads as

$$\mathcal{L}_{eff} = \frac{G_F}{\sqrt{2}} V_{cb} \bar{\ell} \gamma^\mu (1 - \gamma_5) \nu_\ell \bar{c} \gamma_\mu (1 - \gamma_5) b, \quad (1)$$

in which,

$$\begin{aligned} \mathcal{M} &= \frac{G_F}{\sqrt{2}} V_{cb} \langle D_s^{(*)} | \bar{c} \mathcal{O}^\mu b | B_s \rangle \ell^+ \mathcal{O}_\mu \nu_\ell \\ &= \frac{G_F}{\sqrt{2}} V_{cb} H^\mu L_\mu, \end{aligned} \quad (2)$$

where $\mathcal{O}^\mu = \gamma^\mu (1 - \gamma_5)$, and G_F is the Fermi coupling constant. In the electroweak current $\langle D_s | (V - A)_\mu | B_s \rangle$, the vector component is $V_\mu = \bar{b} \gamma_\mu c$ and $A_\mu = \bar{b} \gamma_5 \gamma_\mu c$ is the axial vector one. In the amplitude of $B_s \rightarrow D_s$, only the vector component contributes, because axial vector one fails to meet the property of parity invariance of QCD. The transition of $B_s \rightarrow D_s \ell^+ \nu_\ell$ in terms of form factors can be written as

$$\langle D_s(p_2) | V_\mu | B_s(p_1) \rangle = (P_\mu - \frac{m_1^2 - m_2^2}{q^2} q_\mu) F_1(q^2) + \frac{m_1^2 - m_2^2}{q^2} q_\mu F_0(q^2), \quad (3)$$

where p_1, p_2, m_1 , and m_2 are the four-momentum of B_s, D_s , and their masses respectively. P_μ and q_μ are explained as $P_\mu = (p_1 + p_2)_\mu$ and $q_\mu = (q_1 + q_2)_\mu$. For the transition of $B_s \rightarrow D_s^* \ell^+ \nu_\ell$, one can write

$$\langle D_s^*(p_2) | V_\mu - A_\mu | B_s(p_1) \rangle = \epsilon_2^{\dagger\nu} T_{\mu\nu}, \quad (4)$$

with ϵ_2 the polarization vector of the vector meson D_s^* and one has

$$\begin{aligned} T_{\mu\nu} &= -(m_1 + m_2) [g_{\mu\nu} - \frac{P_\nu}{q^2} q_\mu] A_1(q^2) + \frac{P_\nu}{m_1 + m_2} [P_\mu - \frac{m_1^2 - m_2^2}{q^2} q_\mu] A_2(q^2) \\ &\quad - 2m_2 \frac{P_\nu}{q^2} q_\mu A_0(q^2) + \frac{i}{m_1 + m_2} \epsilon_{\mu\nu\alpha\beta} P^\alpha q^\beta V(q^2). \end{aligned} \quad (5)$$

The Levi-Civita tensor in Minkowski space is $\epsilon_{0123} = +1$. For $B_s \rightarrow D_s^*$, the hadronic tensor can be written as [19]

$$H^{\mu\nu} = T_{\mu\alpha} T_{\nu\beta}^\dagger (-g^{\alpha\beta} + \frac{p_2^\alpha p_2^\beta}{m_2^2}), \quad (6)$$

in which we consider $H_\mu = \epsilon_2^{*\alpha} T_{\mu\alpha}$, $|p_2|$ the momentum of the $W_{\text{off-shell}}$ and the relation between polarization vectors $\epsilon^\mu \epsilon^{*\nu} = -g^{\mu\nu} + \frac{p_2^\mu p_2^\nu}{m_2^2}$.

In the helicity space, the hadronic tensor is given by

$$H(\lambda_W, \lambda'_W) = \epsilon^{\dagger\mu}(\lambda_W) \epsilon^\nu(\lambda'_W) H_{\mu\nu} = H_{\lambda_W} H_{\lambda'_W}^\dagger, \quad (7)$$

for $B_s \rightarrow D_s$ using $H_{\lambda_W} = \epsilon^{\dagger\mu}(\lambda_W) T_\mu$ in which λ_W describes the polarization index of $W_{\text{off-shell}}$. In the helicity basis of $\epsilon^\mu(\lambda_W)$, there are an orthonormal and complete polarization vectors with three spin-1 components having the relation with momentum transfer

$\epsilon^\mu(\lambda_W)q_\mu = 0$ in the cases of $\lambda_W = 0, \pm$, and $\epsilon^\mu(t) = q_\mu/\sqrt{q^2}$ with one spin-0 component $\lambda_W = t$. The polarization four-vectors have orthonormality and completeness relations

$$\epsilon_\mu(\lambda_W)\epsilon_\nu^\dagger(\lambda'_W)g_{\lambda_W\lambda'_W} = g_{\mu\nu}, \quad (8)$$

and

$$\epsilon_\mu^\dagger(\lambda_W)\epsilon^\mu(\lambda'_W) = g_{\lambda_W\lambda'_W}, \quad (9)$$

with $g_{\mu\nu} = \text{diag}(+, -, -, -)$. Using Eqs. (8, 9) in the helicity component space, the leptonic and hadronic tensors will be contracted as [19, 20]

$$\begin{aligned} L^{\mu\nu}H_{\mu\nu} &= L_{\mu'\nu'}g^{\mu'\mu}g^{\nu'\nu}H_{\mu\nu} \\ &= L_{\mu'\nu'}\epsilon^{\mu'}(\lambda_W)\epsilon^{\dagger\mu}(\lambda''_W)g_{\lambda_W\lambda''_W}\epsilon^{\nu'}(\lambda'_W)\epsilon^\nu(\lambda'''_W)g_{\lambda'_W\lambda'''_W}H_{\mu\nu} \\ &= L(\lambda_W, \lambda'_W)g_{\lambda_W\lambda''_W}g_{\lambda'_W\lambda'''_W}H(\lambda''_W, \lambda'''_W), \end{aligned} \quad (10)$$

with the leptonic and hadronic tensors,

$$L(\lambda_W, \lambda'_W) = \epsilon^{\mu'}(\lambda_W)\epsilon^{\dagger\nu'}(\lambda'_W)L_{\mu'\nu'}, \quad (11)$$

and

$$H(\lambda_W, \lambda'_W) = \epsilon^{\dagger\mu}(\lambda_W)\epsilon^\nu(\lambda'_W)H_{\mu\nu}. \quad (12)$$

In the initial B_s rest frame, the momentum and polarization vectors are defined as

$$\begin{aligned} p_1^\mu &= (m_1, 0), \\ p_2^\mu &= (E_2, 0, 0, -|\vec{p}_2|), \\ q^\mu &= (q_0, 0, 0, |\vec{p}_2|), \end{aligned} \quad (13)$$

with E_2 the energy of the D_s meson, $q_0 = (m_1^2 - m_2^2 + q^2)/2m_1$ and [21]

$$\epsilon^\mu(t) = \frac{1}{\sqrt{q^2}}(q_0, 0, 0, |\vec{p}_2|), \epsilon^\mu(\pm) = \frac{1}{\sqrt{2}}(0, \mp 1, -i, 0), \epsilon^\mu(0) = \frac{1}{\sqrt{q^2}}(|\vec{p}_2|, 0, 0, q_0). \quad (14)$$

Applying Eqs. (3) and (14), one obtains the helicity amplitudes with respect of form factors

$$H_t = \frac{1}{\sqrt{q^2}}(m_1^2 - m_2^2)F_0(q^2), \quad H_\pm = 0, \quad H_0 = \frac{1}{\sqrt{q^2}}(2m_1|\vec{p}_2|)F_1(q^2). \quad (15)$$

For the transition of $B_s \rightarrow D_s^*$, the hadronic tensor can be written as [20]

$$H(\lambda_W, \lambda'_W) = \epsilon^{\dagger\mu}(\lambda_W)\epsilon^\nu(\lambda'_W)H_{\mu\nu} = H_{\lambda_W\lambda_V}H_{\lambda'_W\lambda_V}^\dagger, \quad (16)$$

where $H_{\lambda_W\lambda_V}$ is considered as

$$H_{\lambda_W\lambda_V} = \epsilon^{\dagger\mu}(\lambda_W)\epsilon_2^{\dagger\alpha}(\lambda_V)T_{\mu\alpha}. \quad (17)$$

The angular momentum conservation requires that $\lambda_V = \lambda_W, \lambda'_V = \lambda'_W$ when $\lambda_W, \lambda'_W = \pm, 0$ and $\lambda_V, \lambda'_V = 0$ while $\lambda_W, \lambda'_W = t$. In the initial meson rest frame, the polarization four-vectors of D_s^* vector meson $\epsilon_2^\mu(\lambda_V)$ can be determined by

$$\epsilon_2^\mu(\pm) = \frac{1}{\sqrt{2}}(0, \pm 1, -i, 0), \epsilon_2^\mu(0) = \frac{1}{m_2}(|\vec{p}_2|, 0, 0, -E_2). \quad (18)$$

with the helicity components basis. Employing Eqs. (5) and (18), one finds the corresponding helicity amplitudes of $B_s \rightarrow D_s^*$

$$\begin{aligned}
H_t &= -\frac{2m_1|\vec{p}_2|}{\sqrt{q^2}}A_0(q^2), \\
H_{\pm} &= -(m_1 + m_2)A_1(q^2) \pm \frac{2m_1|\vec{p}_2|}{m_1 + m_2}V(q^2) \\
H_0 &= -\frac{m_1 + m_2}{2m_2\sqrt{q^2}}(m_1^2 - m_2^2 - q^2)A_1(q^2) + \frac{2m_1^2|\vec{p}_2|^2}{(m_1 + m_2)(m_2\sqrt{q^2})}A_2(q^2).
\end{aligned} \tag{19}$$

B. Twofold angular distribution

The twofold differential decay distribution versus the momentum transfer q^2 and polar angle θ , which is the angle between the momentum of lepton and the momentum of daughter's meson in the rest frame of $W_{\text{off-shell}}$, can be written as

$$\frac{d^2\Gamma(B_s \rightarrow D_s^{(*)}l^+\nu_l)}{dq^2 d\cos\theta} = \frac{G_F^2|V_{cb}|^2}{(2\pi)^3} \frac{|\vec{p}_2|}{64m_1^2} \left(1 - \frac{m_\ell^2}{q^2}\right) H^{\mu\nu}L_{\mu\nu}, \tag{20}$$

where hadronic tensor parts can be obtained by Eqs. (7, 16) for $B_s \rightarrow D_s$ and $B_s \rightarrow D_s^{(*)}$ respectively. In the W rest frame, leptonic tensor can be explained as

$$L_{\mu\nu} = \text{Tr}[(\not{k}_1 + m_l)\mathcal{O}_\mu\not{k}_2\mathcal{O}_\nu], \tag{21}$$

for $W^- \rightarrow \ell^-\bar{\nu}_\ell$, and

$$L_{\mu\nu} = \text{Tr}[(\not{k}_1 - m_l)\mathcal{O}_\nu\not{k}_2\mathcal{O}_\mu], \tag{22}$$

for the case of $W^+ \rightarrow \ell^+\nu_\ell$. They can be written in the following formula

$$L_{\mu\nu} = 8(k_1^\mu k_2^\nu + k_1^\nu k_2^\mu - k_1 \cdot k_2 g^{\mu\nu} \pm i\varepsilon^{\mu\nu\alpha\beta} k_{1\alpha} k_{2\beta}), \tag{23}$$

where

$$\begin{aligned}
q^\mu &= (\sqrt{q^2}, 0, 0, 0), \\
k_1^\mu &= (E_1, |\vec{k}_1| \sin\theta \cos\chi, |\vec{k}_1| \sin\theta \sin\chi, |\vec{k}_1| \cos\theta), \\
k_2^\mu &= (|\vec{k}_1|, -|\vec{k}_1| \sin\theta \cos\chi, -|\vec{k}_1| \sin\theta \sin\chi, -|\vec{k}_1| \cos\theta),
\end{aligned} \tag{24}$$

with the energy $E_1 = \frac{q^2 + m_\ell^2}{2\sqrt{q^2}}$, and three-momentum of the charged lepton $|\vec{k}_1| = \frac{q^2 - m_\ell^2}{2\sqrt{q^2}}$. We need to define the polarization vectors in the W rest frame to find the leptonic tensor elements. They have longitudinal, transverse, and time helicity components as

$$\begin{aligned}
\epsilon^\mu(\pm 1) &= \frac{1}{\sqrt{2}}(0, \mp 1, -i, 0), \\
\epsilon^\mu(0) &= (0, 0, 0, 1), \\
\epsilon^\mu(t) &= (1, 0, 0, 0).
\end{aligned} \tag{25}$$

Substituting Eqs.(11, 25) in Eq. (23), one gets

$$\begin{aligned}
& (2q^2v)^{-1}L(\lambda_W, \lambda'_W)(\theta, \chi) \\
&= \begin{pmatrix} 0 & 0 & 0 & 0 \\ 0 & (1 \mp \cos \theta)^2 & \mp \frac{2}{\sqrt{2}}(1 \mp \cos \theta) \sin \theta e^{i\chi} & \sin^2 \theta e^{2i\chi} \\ 0 & \mp \frac{2}{\sqrt{2}}(1 \mp \cos \theta) \sin \theta e^{-i\chi} & 2\sin^2 \theta & \mp \frac{2}{\sqrt{2}}(1 \pm \cos \theta) \sin \theta e^{i\chi} \\ 0 & \sin^2 \theta e^{-2i\chi} & \mp \frac{2}{\sqrt{2}}(1 \pm \cos \theta) \sin \theta e^{-i\chi} & (1 \pm \cos \theta)^2 \end{pmatrix} \quad (26) \\
&+ \delta_\ell \begin{pmatrix} 4 & -\frac{4}{\sqrt{2}} \sin \theta e^{-i\chi} & 4 \cos \theta & \frac{4}{\sqrt{2}} \sin \theta e^{i\chi} \\ -\frac{4}{\sqrt{2}} \sin \theta e^{i\chi} & 2\sin^2 \theta & -\frac{2}{\sqrt{2}} \sin 2\theta e^{i\chi} & -2\sin^2 \theta e^{2i\chi} \\ 4 \cos \theta & -\frac{2}{\sqrt{2}} \sin 2\theta e^{-i\chi} & 4\cos^2 \theta & \frac{2}{\sqrt{2}} \sin 2\theta e^{i\chi} \\ \frac{4}{\sqrt{2}} \sin \theta e^{-i\chi} & -2\sin^2 \theta e^{-2i\chi} & \frac{2}{\sqrt{2}} \sin 2\theta e^{-i\chi} & 2\sin^2 \theta \end{pmatrix},
\end{aligned}$$

with velocity-type $v = 1 - m_\ell^2/q^2$ and $\delta_\ell = m_\ell^2/2q^2$ helicity-flip factors, and the upper/lower sign refers to the two configurations $\ell^- \bar{\nu}_\ell / \ell^+ \nu_\ell$. Integrating over the azimuthal angle χ , Eq. (26) becomes

$$\begin{aligned}
& \frac{1}{2\pi} (2q^2v)^{-1}L(\lambda_W, \lambda'_W)(\theta) \\
&= \begin{pmatrix} 0 & 0 & 0 & 0 \\ 0 & (1 \mp \cos \theta)^2 & 0 & 0 \\ 0 & 0 & 2\sin^2 \theta & 0 \\ 0 & 0 & 0 & (1 \pm \cos \theta)^2 \end{pmatrix} \quad (27) \\
&+ \delta_\ell \begin{pmatrix} 4 & 0 & 4 \cos \theta & 0 \\ 0 & 2\sin^2 \theta & 0 & 0 \\ 4 \cos \theta & 0 & 4\cos^2 \theta & 0 \\ 0 & 0 & 0 & 2\sin^2 \theta \end{pmatrix}.
\end{aligned}$$

We continue with the lower sign in the matrix since it is our study case $B_s \rightarrow D_s^{(*)} \ell^+ \nu_\ell$. Therefore, the twofold polar angular distribution becomes [21]

$$\begin{aligned}
\frac{d\Gamma(B_s \rightarrow D_s^{(*)} \ell^+ \nu_\ell)}{dq^2 d\cos \theta} &= \frac{G_F^2 |V_{cb}|^2 |\vec{p}_2|^2 q^2 v^2}{32(2\pi)^3 m_1^2} \times \{(1 + \cos^2 \theta) \mathcal{H}_U + 2\sin^2 \theta \mathcal{H}_L + 2\cos \theta \mathcal{H}_P \\
&+ 2\delta_\ell [\sin^2 \theta \mathcal{H}_U + 2\cos^2 \theta \mathcal{H}_L + 2\mathcal{H}_S - 4\cos \theta \mathcal{H}_{SL}]\}, \quad (28)
\end{aligned}$$

with the following helicity structure functions

$$\begin{aligned}
\mathcal{H}_U &= |H_+|^2 + |H_-|^2, \quad \mathcal{H}_L = |H_0|^2, \quad \mathcal{H}_S = |H_t|^2, \\
\mathcal{H}_P &= |H_+|^2 - |H_-|^2, \quad \mathcal{H}_{SL} = \text{Re}(H_0 H_t^\dagger). \quad (29)
\end{aligned}$$

Finally, the differential decay distribution over transfer momentum q^2 , is defined as

$$\frac{d\Gamma(B_s \rightarrow D_s^{(*)} \ell^+ \nu_\ell)}{dq^2} = \frac{G_F^2 |V_{cb}|^2 |\vec{p}_2|^2 q^2 v^2}{12(2\pi)^3 m_1^2} \times \mathcal{H}_{tot}, \quad (30)$$

where

$$\mathcal{H}_{tot} = \mathcal{H}_U + \mathcal{H}_L + \delta_\ell [\mathcal{H}_U + \mathcal{H}_L + 3\mathcal{H}_S]. \quad (31)$$

C. Physical observables

In addition to the branching fraction of semileptonic decay $B_s \rightarrow D_s^*$, we can investigate other physical observables. The forward-backward asymmetry is given by [20]

$$A_{FB}^\ell(q^2) = \frac{\int_0^1 d\cos\theta \frac{d\Gamma}{dq^2 d\cos\theta} - \int_{-1}^0 d\cos\theta \frac{d\Gamma}{dq^2 d\cos\theta}}{\int_0^1 d\cos\theta \frac{d\Gamma}{dq^2 d\cos\theta} + \int_{-1}^0 d\cos\theta \frac{d\Gamma}{dq^2 d\cos\theta}} = \frac{3\mathcal{H}_P - 4\delta_\ell \mathcal{H}_{SL}}{4\mathcal{H}_{tot}}. \quad (32)$$

For the longitudinal polarization of the lepton with the following vector

$$s_L^\mu = \frac{1}{m_\ell} (|\vec{k}_1|, E_1 \sin\theta, 0, E_1 \cos\theta), \quad (33)$$

the leptonic tensor is defined as

$$L_{\mu\nu}(s_L) = \mp (s_{L\mu} k_{2\nu} + s_{L\nu} k_{2\mu} - s_L \cdot k_2 g_{\mu\nu} \pm i\varepsilon_{\mu\nu\alpha\beta} s_L^\alpha k_2^\beta), \quad (34)$$

where the upper/lower sign corresponds to the $\ell^- \bar{\nu}_\ell / \ell^+ \nu_\ell$. Then the polarized differential semileptonic decay can be written as

$$\frac{d\Gamma(s_L)}{dq^2} = \frac{G_F^2 |V_{cb}|^2 |\vec{p}_2|^2 q^2 v^2}{12(2\pi)^3 m_1^2} \times [\mathcal{H}_U + \mathcal{H}_L - \delta_\ell (\mathcal{H}_U + \mathcal{H}_L + 3\mathcal{H}_S)]. \quad (35)$$

The ratio of polarized decay distribution to the unpolarized one, Eq. (30), is known as longitudinal polarization of the lepton which can be written [20]

$$P_L^\ell(q^2) = \frac{\mathcal{H}_U + \mathcal{H}_L - \delta_\ell (\mathcal{H}_U + \mathcal{H}_L + 3\mathcal{H}_S)}{\mathcal{H}_{tot}}, \quad (36)$$

for the case $W^+ \rightarrow \ell^+ \nu_\ell$. To get the transverse polarization P_T^ℓ , one can consider $s_T^\mu = (0, \cos\theta, 0, -\sin\theta)$, and the transverse polarization of lepton becomes [20]

$$P_T^\ell(q^2) = \frac{-3\pi\sqrt{\delta_\ell} (\mathcal{H}_P + 2\mathcal{H}_{SL})}{4\sqrt{2} \mathcal{H}_{tot}}. \quad (37)$$

Furthermore, the lepton-side convexity parameter can be defined as [20]

$$C_F^\ell(q^2) = \frac{3}{4} (1 - 2\delta_\ell) \frac{\mathcal{H}_U - 2\mathcal{H}_L}{\mathcal{H}_{tot}}. \quad (38)$$

The longitudinal polarization fractions of the $D_s^{(*)}$ meson is given by [20]

$$F_L^\ell(q^2) = \frac{(1 + \delta_\ell)\mathcal{H}_L + 3\delta_\ell \mathcal{H}_S}{\mathcal{H}_{tot}}. \quad (39)$$

D. $B_s \rightarrow D_s P$ and $B_s \rightarrow D_s V$

The factorization assumption based on the vacuum saturation approximation works reasonably well in analyzing heavy-quark physics. In the factorization approach, the effective Hamiltonian of $B_s \rightarrow D_s P(V)$ can be written as

$$\mathcal{H}_{\text{eff}} = \frac{G_F}{\sqrt{2}} V_{cb} V_{q_1 q_2} (C_1 O_1 + C_2 O_2) + \text{H.c.}, \quad (40)$$

where $V_{q_1 q_2}$ is the corresponding CKM element, $C_{(1,2)}$ are the Wilson coefficients and the local tree four-quark operators are given by [22]

$$\begin{aligned} O_1 &= \bar{q}_{1,\alpha} \gamma_\mu (1 - \gamma_5) c_\alpha \cdot \bar{u}_\beta \gamma^\mu (1 - \gamma_5) q_{2,\beta}, \\ O_2 &= \bar{q}_{1,\alpha} \gamma_\mu (1 - \gamma_5) c_\beta \cdot \bar{u}_\beta \gamma^\mu (1 - \gamma_5) q_{2,\alpha}, \end{aligned} \quad (41)$$

with α, β color indices. Using the effective Hamiltonian, the matrix elements for the decays $B_s \rightarrow D_s P(V)$ become as

$$\begin{aligned} \mathcal{A}(B_s \rightarrow D_s P(V)) &= \langle D_s P(V) | \mathcal{H}_{\text{eff}} | B_s \rangle \\ &= \frac{G_F}{\sqrt{2}} V_{cb} V_{q_1 q_2} a_1 \langle P(V) | J^\mu | 0 \rangle \langle D_s | J_\mu | B_s \rangle, \end{aligned} \quad (42)$$

where a_1 is a QCD factor, defined in terms of the Wilson coefficients as $a_1 = C_2 + C_1/3$. One can write $\langle P | J^\mu | 0 \rangle = -i f_P q_\mu$ and $\langle V | J^\mu | 0 \rangle = f_V m_V \epsilon_\mu^*$ in terms of decay constants of pseudoscalar and vector mesons. Thus, the amplitude for $B_s \rightarrow D_s P$ and $B_s \rightarrow D_s V$ can be specified as follows:

$$\begin{aligned} \mathcal{A}(B_s \rightarrow D_s P) &= \frac{G_F}{\sqrt{2}} V_{cb} V_{q_1 q_2} a_1 (m_1^2 - m_2^2) f_P f_0^{B_s D_s} (m_P^2), \\ \mathcal{A}(B_s \rightarrow D_s V) &= \sqrt{2} G_F V_{cb} V_{q_1 q_2} a_1 m_V (\epsilon_V^* \cdot p_{B_s}) f_V f_+^{B_s D_s} (m_V^2), \end{aligned} \quad (43)$$

with regard to the decay constants and transition form factors. The corresponding expressions for the decay width of these two-body decays can be written as [23]

$$\begin{aligned} \Gamma(B_s \rightarrow D_s P) &= \frac{p}{8\pi m_1^2} |\mathcal{A}|^2, \\ \Gamma(B_s \rightarrow D_s V) &= \frac{p}{8\pi m_1^2} \sum_{\text{pol}} |\mathcal{A}|^2 \end{aligned} \quad (44)$$

with p the momentum of either meson in the final state, $p = p_{D_s} = p_{P/V} = \sqrt{(m_1^2 - (m_2 + m_{P/V})^2)(m_1^2 - (m_2 - m_{P/V})^2)}/2m_1$ in the center-of-mass frame.

E. Form factors

To calculate the physical observables of semileptonic decays, the transition form factors and their dependence on transfer momentum should be known. The transition hadronic form factors are also important in nonleptonic decays. There are numerous models available to describe them. Some of them such as perturbative predictions are limited to a region of small

values of q^2 . Lattice QCD results are also reliable close to zero recoil, the reason originating from avoiding large statistical errors. In the current work, we make the extrapolation by using two formulations, dipole and exponential functions as follows [22–24]

$$F(q^2) = \frac{F(0)}{1 - a_1 \frac{q^2}{m_{pole}^2} + a_2 \frac{q^4}{m_{pole}^4}}, \quad (45)$$

$$F(q^2) = F(0) \exp[a_1 q^2 + a_2 q^4],$$

where $F(0)$, a_1 , a_2 are free parameters in both equations obtained by performing fit. $F(q^2)$ stands for the form factors $f_{0,+}(q^2)$, $A_{0,1,2}(q^2)$, $V(q^2)$ and m_{pole} is the mass of the pole. The input parameters are identified in the next section.

III. NUMERICAL ANALYSIS

In this section, we first discuss $B_s \rightarrow D_s \ell \nu$ and its numerical observables. After that, $B_s \rightarrow D_s^* \ell \nu$ are investigated. In the computational evaluations, the following inputs are employed [25]:

$$\begin{aligned} m_{B_{c0}} &= 6.704 \text{ GeV}, m_{B_c^*} = 6.329 \text{ GeV}, m_{B_s} = 5.3669 \text{ GeV}, \\ m_{D_s} &= 1.9683 \text{ GeV}, m_e = 0.511 \text{ MeV}, m_\mu = 105.658 \text{ MeV}, \\ m_\tau &= 1.777 \text{ GeV}, \tau_{B_s} = 1.527 \text{ ps}, m_{D_s^*} = 2.112 \text{ GeV}, \\ f_{D_s} &= 249.9 \text{ MeV}, f_{K^+} = 155.7 \text{ MeV}, f_{K^*} = 0.217 \text{ GeV}, \\ f_\rho &= 0.209 \text{ GeV}, f_{D_s^*} = 0.315 \text{ GeV}, f_{\pi^+} = 130.2 \text{ MeV}, \\ V_{cb} &= 0.0408, V_{cs} = 0.975, V_{ud} = 0.974, V_{us} = 0.224. \end{aligned}$$

In Ref. [17], HPQCD collaboration presented a lattice QCD determination of the $B_s \rightarrow D_s \ell \nu$ using the BCL parametrization [26] for the form factors. We used their mean values and the covariance matrix associated with the parameters in the BCL formulation to perform the fitting in the transition of $B_s \rightarrow D_s \ell \nu$. Our results are shown in Figs. 1, 2, 3, 4 for the dipole and exponential models respectively. Figs. 2 and 4 show the covariance between our obtained parameters for $F(0)$, a_1 and a_2 . In the dipole form, they are larger. In Table I, we present the calculated parameters $F(0)$, a_1 , and a_2 for f_0 and f_+ in both models. As one can see, the values of $F(0)$ are near in both formulations, however, a_1 and a_2 have more different values. The average of χ^2 in the dipole model is obtained as 0.1437 and equal to 0.0483 for the exponential one. By using the obtained parameters in Table I, we tabulate the decay rates of semileptonic transitions of $B_s \rightarrow D_s \ell \nu$ in Table II. Our predictions of $BR(B_s \rightarrow D_s \mu \nu)$, $BR(B_s \rightarrow D_s e \nu)$, and $BR(B_s \rightarrow D_s \tau \nu)$ are close to the QCD sum rules approaches, $BR(B_s \rightarrow D_s \ell \nu) = 2.03_{-0.49}^{+0.35}$ [27] and $BR(B_s \rightarrow D_s \tau \nu) = 0.606_{-0.211}^{+0.266}$ [6]. The semi-muonic channel was reported by PDG as $BR(B_s^0 \rightarrow D_s^- \mu^+ \nu_\mu) = (2.31 \pm 0.21)\%$ [25]. Our values, $(2.3065 \pm 0.9503)\%$ and $(2.3084 \pm 0.9513)\%$ are both in good agreement with them. By employing of equations related to physical observables in section II C, we can obtain forward-backward asymmetry, longitudinal, transverse lepton polarization, and leptonic convexity parameters for different leptonic channels of $B_s \rightarrow D_s \ell \nu$, see Tables III and IV. The longitudinal polarization of the lepton τ had been reported as 0.30 in PQCD approach [7]. Our magnitude of this observable is near with them.

For the semileptonic $B_s \rightarrow D_s^*$, vector and axial-vector form factors have been computed by HPQCD Collaboration using lattice QCD [18] with z -expansion parameterization with

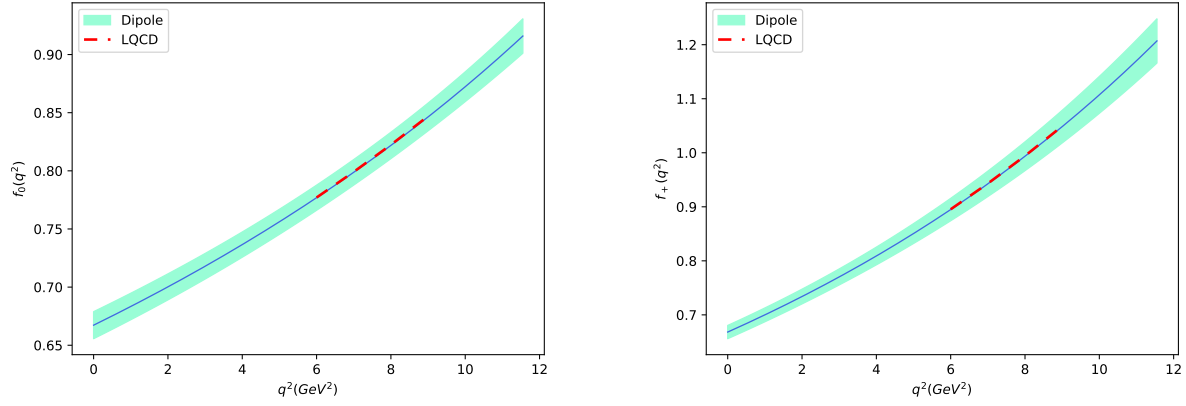


FIG. 1: The fitted form factors f_0 and f_+ versus q^2 using dipole model.

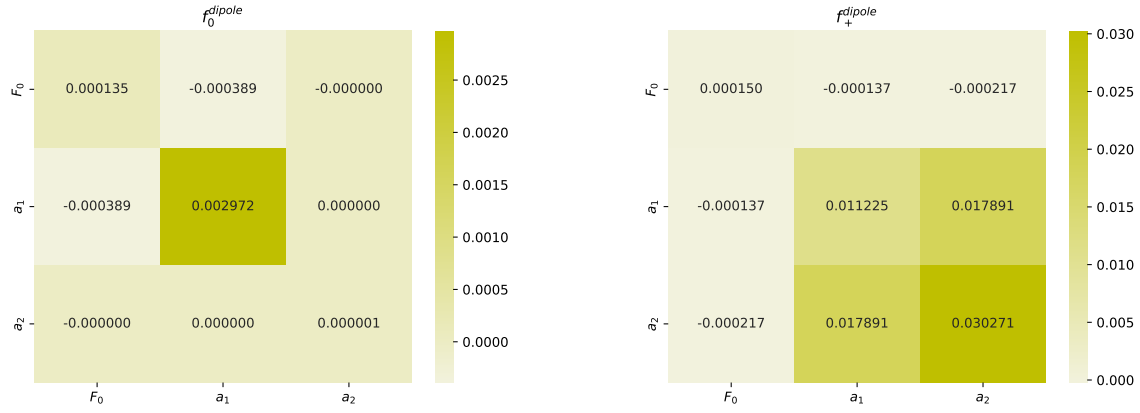


FIG. 2: The covariance of parameters in the dipole form factors f_0 and f_+ .

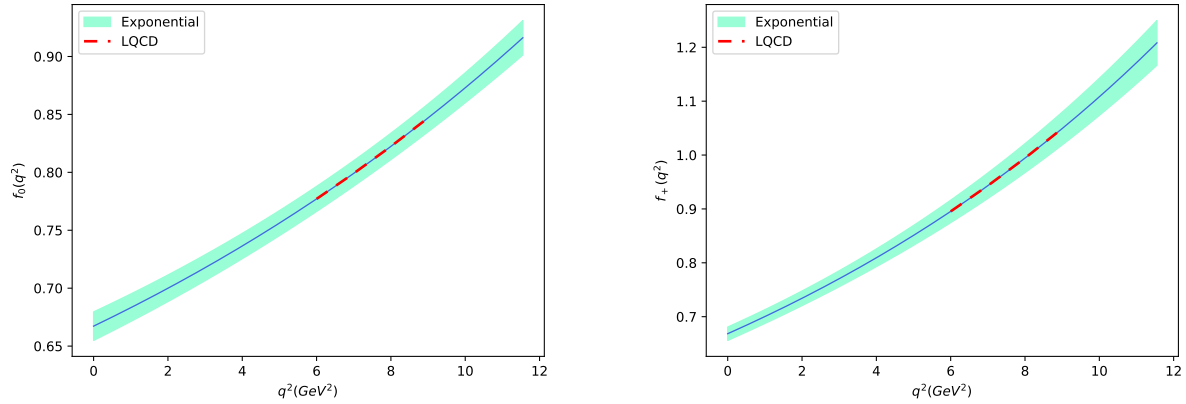


FIG. 3: The fitted form factors f_0 and f_+ versus q^2 using exponential model.

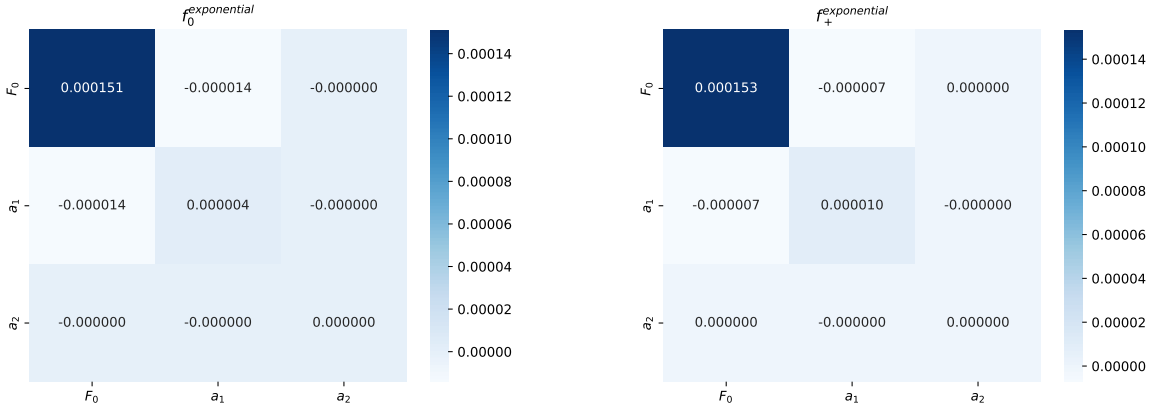


FIG. 4: The covariance of parameters in the exponential form factors f_0 and f_+ .

TABLE I: Fitted parameters $F(0)$, a_1 , and a_2 for f_0 and f_+ in transition of $B_s \rightarrow D_s$.

	$f_0^{dipole}(q^2)$	$f_0^{exponential}(q^2)$	$f_+^{dipole}(q^2)$	$f_+^{exponential}(q^2)$
$F(0)$	0.6673 ± 0.0116	0.6672 ± 0.0123	0.6682 ± 0.0122	0.6684 ± 0.0124
a_1	1.0574 ± 0.0545	0.0232 ± 0.0019	1.8461 ± 0.1059	0.0460 ± 0.0032
a_2	0.0040 ± 0.0020	0.0004 ± 0.0000	1.0333 ± 0.1740	0.0005 ± 0.0000

three parameters. We have used their mean values and correlation matrices to fit with the form factors of $B_s \rightarrow D_s^*$, $V(q^2)$, $A_{0,1,2}(q^2)$. In Figs. 5, 6, 7, 8, the results associated to the fitting procedure are plotted. As can be seen from Figs. 5 and 7, the behavior of the dipole model is more appropriate than exponential, especially in the case of $A_2(q^2)$. Moreover, the covariances between parameters of the dipole are larger than other ones, see Figs. 6 and 8. In Table V, we report the values of $F(0)$, a_1 , a_2 for the current transition. Using these values in the form factors as well as the helicity amplitudes in Eq. (19), and the differential decay distribution, Eq. (30), one can evaluate the decay rates of $B_s \rightarrow D_s^* \ell \nu$ for semi-electronic, semi-muonic, and semi-tauonic channels in Table VI. For the semi-muonic channel, our values, $(5.2246 \pm 0.4624)\%$ and $(5.2386 \pm 0.4452)\%$ agree well with the PDG data $BR(B_s^0 \rightarrow D_s^{*-} \mu^+ \nu_\mu) = (5.2 \pm 0.5)\%$ [25]. In Ref. [28], the authors obtained 1.35% for the branching fraction of the decay $B_s \rightarrow D_s \ell \nu$. Based on the polarized differential decay,

TABLE II: Decay widths in $10^{(-15)}$ GeV and branching ratios in percentage for semileptonic transition of $B_s \rightarrow D_s \ell \nu_\ell$.

Mode	Γ with dipole	Γ with exponential	BR with dipole	BR with exponential
$B_s^0 \rightarrow D_s^- \mu^+ \nu_\mu$	9.9374 ± 4.0941	9.9455 ± 4.0988	2.3065 ± 0.9503	2.3084 ± 0.9513
$B_s^0 \rightarrow D_s^- e^+ \nu_e$	9.9704 ± 0.0002	9.9786 ± 0.0002	2.3142 ± 0.0000	2.3161 ± 0.0000
$B_s^0 \rightarrow D_s^- \tau^+ \nu_\tau$	2.9643 ± 0.0180	2.9675 ± 0.0180	0.6880 ± 0.0042	0.6888 ± 0.0042

TABLE III: Forward-backward asymmetry for semileptonic transition of $B_s \rightarrow D_s \ell \nu_\ell$.

	$\langle \mathcal{A}_{FB}^e \rangle$	$\langle \mathcal{A}_{FB}^\mu \rangle$	$\langle \mathcal{A}_{FB}^\tau \rangle$
dipole	-0.5175×10^{-6}	-0.0138	-0.3604
exponential	-0.5171×10^{-6}	-0.0138	-0.3604

 TABLE IV: Longitudinal, transverse lepton polarization and leptonic convexity parameters for semileptonic transition of $B_s \rightarrow D_s \ell \nu_\ell$.

	$\langle P_L^e \rangle$	$\langle P_L^\mu \rangle$	$\langle P_T^e \rangle$	$\langle P_T^\mu \rangle$	$\langle P_T^\tau \rangle$	$\langle C_F^e \rangle$	$\langle C_F^\mu \rangle$	$\langle C_F^\tau \rangle$	
dipole	1.0000	0.9611	-0.3211	-0.0010	-0.1975	-0.8419	-1.5000	-1.4574	-0.2702
exp	1.0000	0.9611	-0.3209	-0.0010	-0.1974	-0.8419	-1.5000	-1.4574	-0.2703

the longitudinal and transverse polarizations, the lepton convexity and the longitudinal polarization of a vector meson D_s^* in section II C can be obtained, we report the results for the mentioned quantities in addition to the average of forward-backward asymmetries in Tables VII, VIII. The observable F_L^T for vector meson D_s^* were reported 0.433 and 0.43 in Refs [7, 29] respectively. Our values for longitudinal polarization of D_s^* in Table VII, 0.4401 and 0.4391, are close to them. We apply our results to find the ratio

$$\frac{\Gamma(B_s^0 \rightarrow D_s^- \mu^+ \nu_\mu)}{\Gamma(B_s^0 \rightarrow D_s^{*-} \mu^+ \nu_\mu)} = 0.4415 \pm 0.1860, \quad (46)$$

with the dipole parametrization and

$$\frac{\Gamma(B_s^0 \rightarrow D_s^- \mu^+ \nu_\mu)}{\Gamma(B_s^0 \rightarrow D_s^{*-} \mu^+ \nu_\mu)} = 0.4406 \pm 0.1854, \quad (47)$$

with the exponential one. Those are acceptable when compared with the reported measurement value of 0.464(45) by LHCb collaboration [3]. Moreover, another important quantity is the ratio of $R(D_s)$, using in the lepton universality with an interesting picture emerging, which is calculated as

$$R(D_s) = \frac{BR(B_s^0 \rightarrow D_s^- \tau^+ \nu_\tau)}{BR(B_s^0 \rightarrow D_s^- \mu^+ \nu_\mu)} = 0.2983 \pm 0.1229 \quad (48)$$

with the dipole formula and

$$R(D_s) = \frac{BR(B_s^0 \rightarrow D_s^- \tau^+ \nu_\tau)}{BR(B_s^0 \rightarrow D_s^- \mu^+ \nu_\mu)} = 0.2984 \pm 0.1230 \quad (49)$$

with the exponential formula. Zhang *et al.*, reported $R(D_s) = 0.334 \pm 0.017$ for this quantity and also found the form factors of $B_s \rightarrow D_s$ at the largest recoil point, $f_{+,0}^{B_s \rightarrow D_s}(0) = 0.533_{-0.094}^{+0.112}$ [6]. Ours, $f_{+,0}^{B_s \rightarrow D_s}(0) = 0.67 \pm 0.01$, is in consistent with them. The ratio $R(D_s) = 0.320_{-0.009}^{+0.009}$ was also reported in Ref. [13]. Another ratio which may measured by various groups, is $R(D_s^*)$. We obtain that in both models such that

$$R(D_s^*) = 0.2503 \pm 0.0232 \text{ (dipole)}, R(D_s^*) = 0.2491 \pm 0.0223 \text{ (exponential)}. \quad (50)$$

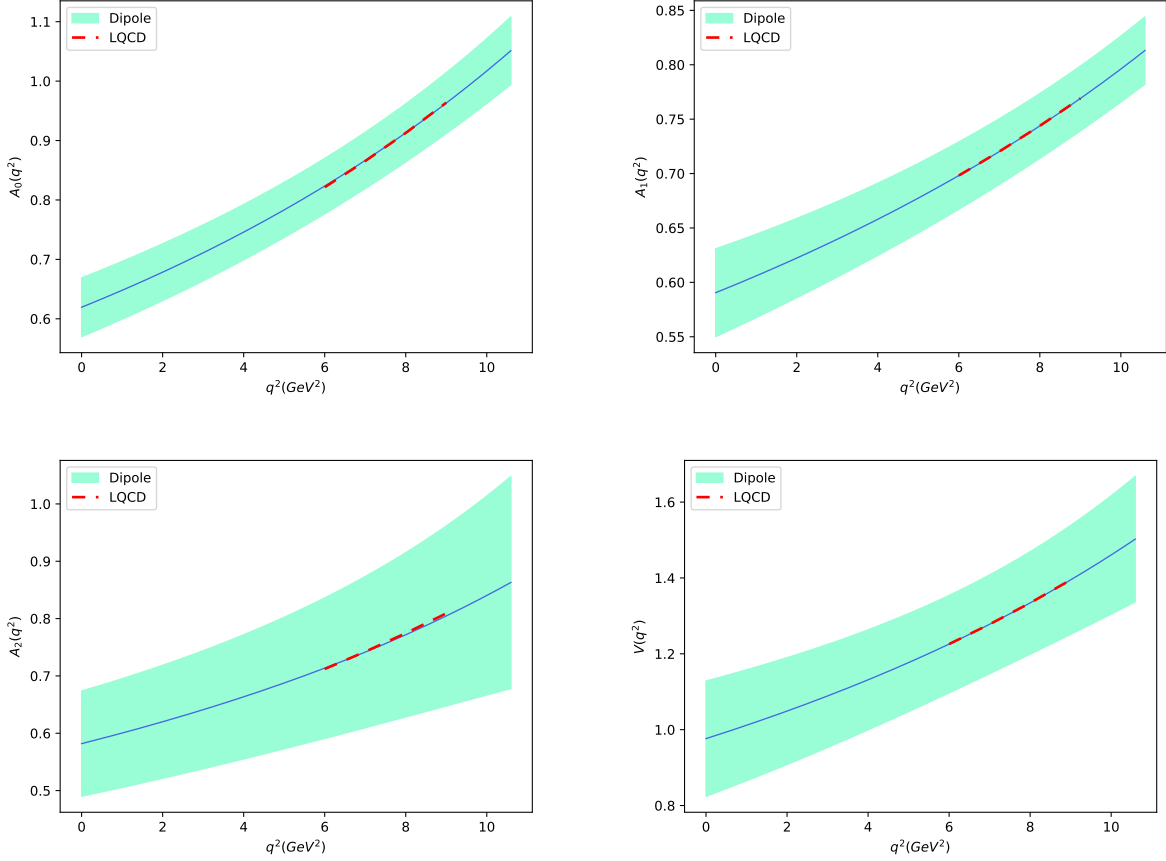


FIG. 5: Form factor fits to LQCD data for transition $B_s \rightarrow D_s^*$ using dipole formula.

This quantity was found to be $R(D_s^*) = 0.2490(60)(35)$ within the Lattice QCD formalism [18]. Moreover, Zhou *et al.*, obtained $R(D_s^*) = 0.251_{-0.003}^{+0.002}$ using Bethe–Salpeter method [13].

Using our form factors in the dipole case, we can construct helicity amplitudes with their error bands. They are plotted in Figs. 9, 10 for $B_s \rightarrow D_s$ and $B_s \rightarrow D_s^*$ respectively. Our helicity amplitudes for $B_s \rightarrow D_s^*$ are equivalent to those in Ref. [18] times a minus sign. At large value of q^2 , H_0, H_{\pm} will be equal. Also, H_0 and H_t have a singularity at $q^2 = 0$ as one would expect from their relations for both transitions $B_s \rightarrow D_s$ and $B_s \rightarrow D_s^*$. The differential decay rates for $B_s \rightarrow D_s \mu \nu$ and $B_s \rightarrow D_s \tau \nu$ are compared in Fig. 11. The dashed lines are associated with the central values and the blue and green bands represent their errors. Fig. 12 show the behaviour of $\frac{d\Gamma}{dq^2}$ for $B_s^0 \rightarrow D_s^{*-} \ell^+ \nu_{\ell}$, where $\ell = \mu, \tau$ as a function of q^2 . The q^2 dependence of the forward-backward asymmetries, the leptonic longitudinal and transverse polarizations are shown in Figs. 13 and 14 for both transitions. At the zero recoil point ($q^2 = q_{max}^2$), \mathcal{A}_{FB} and P_T in Fig. 14, will be zero as one would expect from their relations.

Furthermore, in Table IX, we give the predictions for the branching ratios of two body nonleptonic decays of B_s to a D_s meson along with a pseudoscalar or vector in their final states. The results are compared with PDG [25], factorization approach [30], and quark models [8, 31].

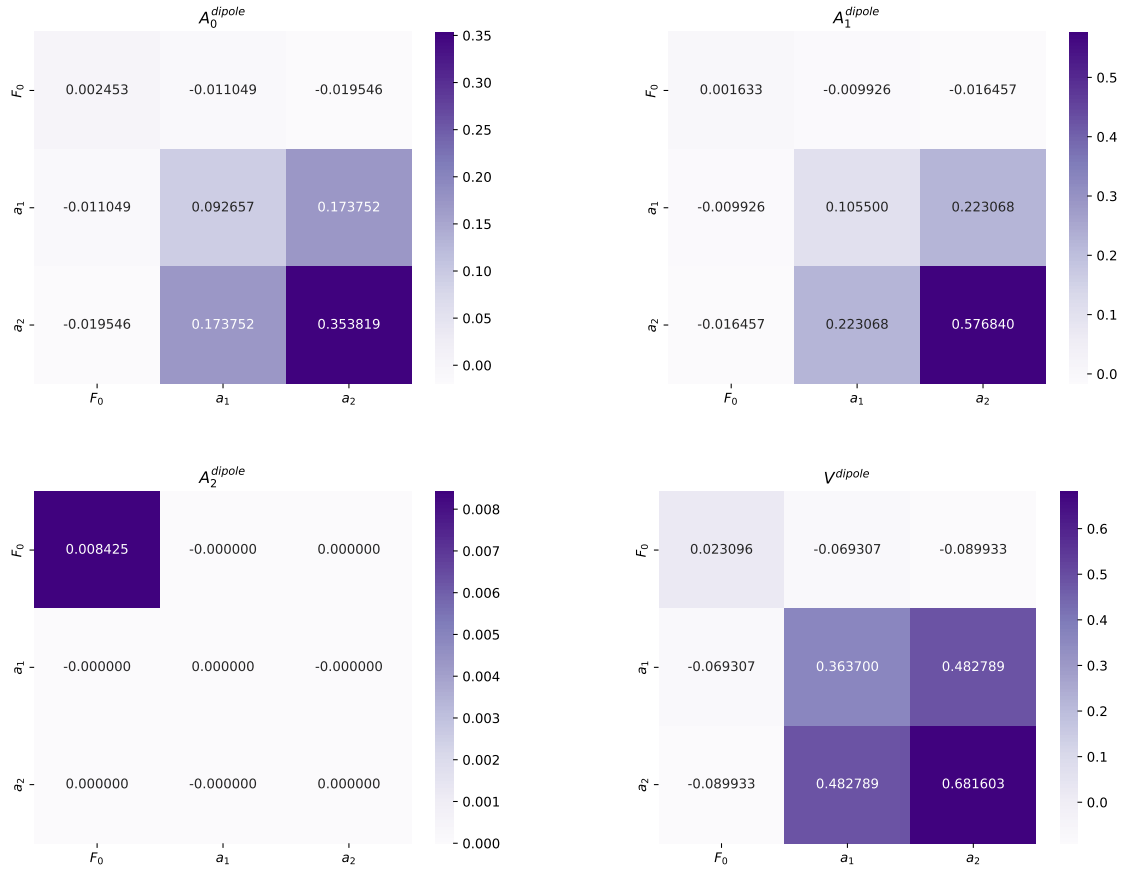


FIG. 6: The covariance of parameters in the dipole form factors V, A_0, A_1, A_2 .

IV. CONCLUSIONS

We have provided a detailed helicity analysis of semileptonic decays $B_s \rightarrow D_s^{(*)} \ell \nu$. Two parameterizations, dipole and exponential, have been considered for the form factors of these weak decays. We have performed fitting to the LQCD data [18] and [17], and obtained free parameters as well as their covariances. We have applied the form factors to obtain the two body nonleptonic decays $B_s \rightarrow D_s + P(V)$. The q^2 dependence of decay widths and physical observables have been plotted. The branching fractions, forward-backward asymmetry, longitudinal and transverse polarizations of the charged lepton as well as the vector meson have been calculated. Our obtained branching fractions, especially in the semi-muonic channels, are in good agreement with the PDG data [25].

Acknowledgements

I would like to thank De-Liang Yao for useful discussions. This work is supported by the Fundamental Research Funds for the Central Universities under Contract No. 531118010379.

-
- [1] S. S. Gershtein and M. Y. Khlopov, Pisma Zh. Eksp. Teor. Fiz. **23**, 374 (1976).
[2] M. Y. Khlopov, Sov. J. Nucl. Phys. **28**, 583 (1978).

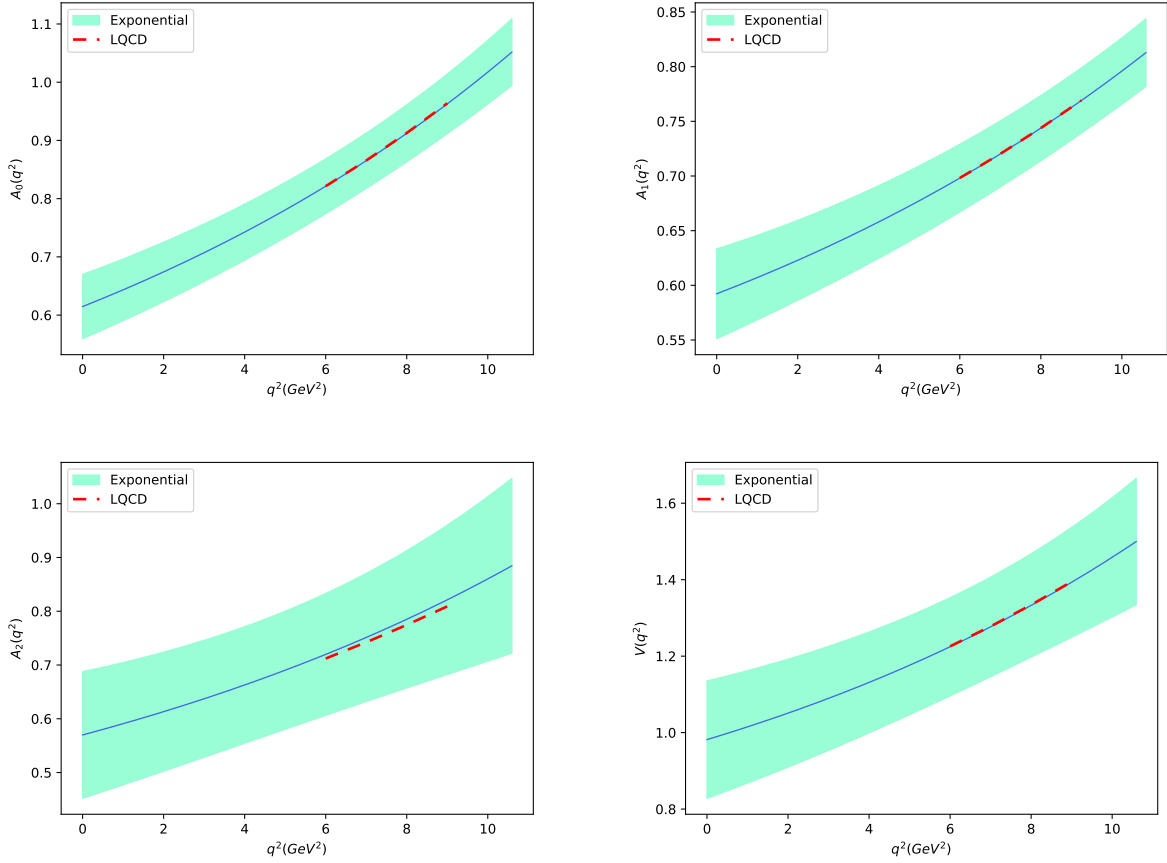


FIG. 7: Form factor fits to LQCD data for transition $B_s \rightarrow D_s^*$ using exponential formula.

- [3] R. Aaij et al. (LHCb), Phys. Rev. D **101**, 072004 (2020), 2001.03225.
- [4] G. Caria et al. (Belle), Phys. Rev. Lett. **124**, 161803 (2020), 1910.05864.
- [5] Y. S. Amhis et al. (HFLAV), Phys. Rev. D **107**, 052008 (2023), 2206.07501.
- [6] Y. Zhang, T. Zhong, H.-B. Fu, W. Cheng, L. Zeng, and X.-G. Wu, Phys. Rev. D **105**, 096013 (2022), 2202.02730.
- [7] X.-Q. Hu, S.-P. Jin, and Z.-J. Xiao, Chin. Phys. C **44**, 053102 (2020), 1912.03981.
- [8] C. Albertus, Few Body Syst. **55**, 1017 (2014), 1403.2719.
- [9] S. Rahmani, W. C. Luo, and C. W. Xiao, Eur. Phys. J. A **59**, 155 (2023), 2212.12933.
- [10] C. W. Xiao, S. Rahmani, and H. Hassanabadi, Eur. Phys. J. Plus **136**, 1083 (2021), 2007.03161.
- [11] S. Rahmani and H. Hassanabadi, Eur. Phys. J. A **53**, 187 (2017).
- [12] S. Rahmani and H. Hassanabadi, Few Body Syst. **58**, 150 (2017).
- [13] T. Zhou, T. Wang, Y. Jiang, X.-Z. Tan, G. Li, and G.-L. Wang, Int. J. Mod. Phys. A **35**, 2050076 (2020), 1910.06595.
- [14] B.-Y. Cui, Y.-K. Huang, Y.-M. Wang, and X.-C. Zhao, Phys. Rev. D **108**, L071504 (2023), 2301.12391.
- [15] N. Rajeev and R. Dutta, Phys. Rev. D **98**, 055024 (2018), 1808.03790.
- [16] N. Das and R. Dutta, Phys. Rev. D **105**, 055027 (2022), 2110.05526.
- [17] E. McLean, C. T. H. Davies, J. Koponen, and A. T. Lytle, Phys. Rev. D **101**, 074513 (2020),

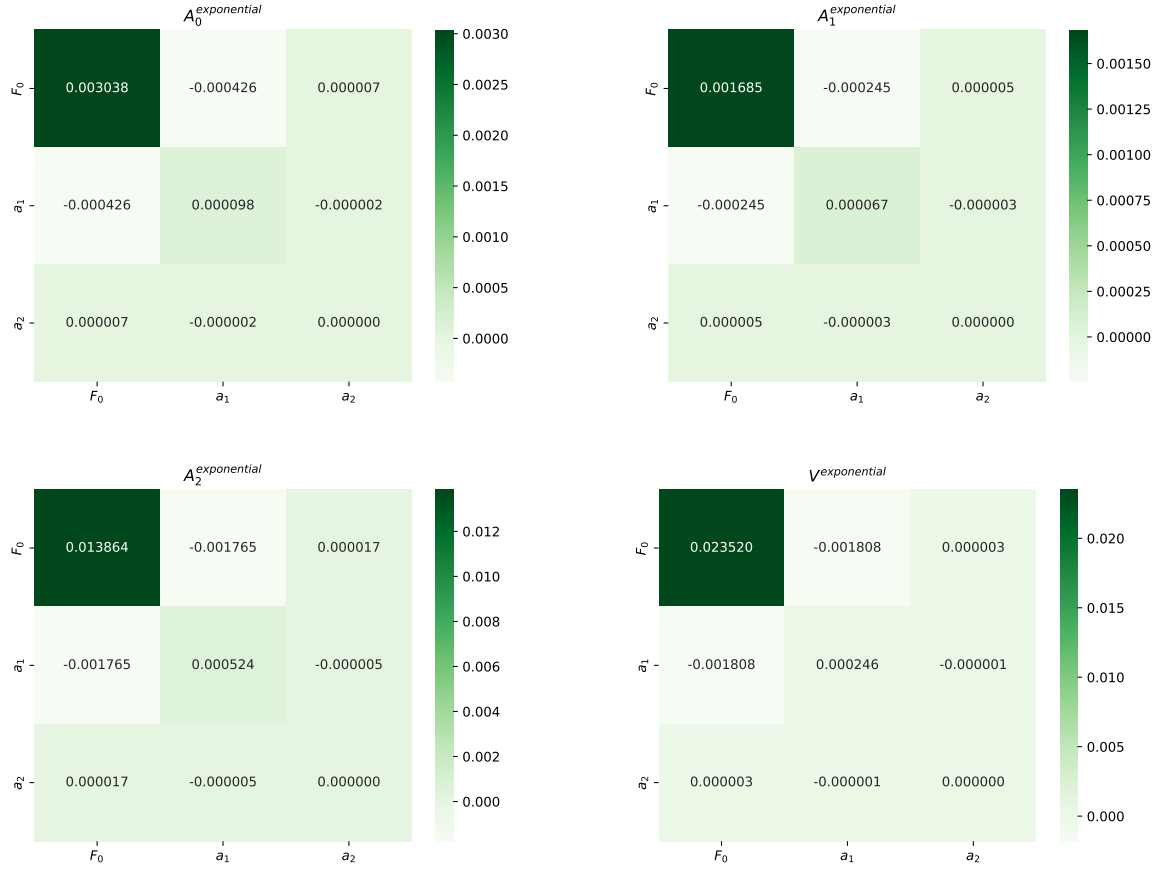


FIG. 8: The covariance of parameters in the exponential form factors V , A_0 , A_1 , A_2 .

1906.00701.

- [18] J. Harrison and C. T. H. Davies (HPQCD), Phys. Rev. D **105**, 094506 (2022), 2105.11433.
- [19] L. Zhang, X.-W. Kang, X.-H. Guo, L.-Y. Dai, T. Luo, and C. Wang, JHEP **02**, 179 (2021), 2012.04417.
- [20] M. A. Ivanov, J. G. Körner, J. N. Pandya, P. Santorelli, N. R. Soni, and C.-T. Tran, Front. Phys. (Beijing) **14**, 64401 (2019), 1904.07740.
- [21] M. A. Ivanov, J. G. Körner, and C. T. Tran, Phys. Rev. D **92**, 114022 (2015), 1508.02678.
- [22] Z.-J. Sun, Z.-Q. Zhang, Y.-Y. Yang, and H. Yang, Eur. Phys. J. C **84**, 65 (2024), 2311.04431.
- [23] Y. Fu-Sheng, X.-X. Wang, and C.-D. Lu, Phys. Rev. D **84**, 074019 (2011), 1101.4714.
- [24] W.-F. Wang, X. Yu, C.-D. Lü, and Z.-J. Xiao, Phys. Rev. D **90**, 094018 (2014), 1401.0391.
- [25] S. Navas et al. (Particle Data Group), Phys. Rev. D **110**, 030001 (2024).
- [26] C. Bourrely, I. Caprini, and L. Lellouch, Phys. Rev. D **79**, 013008 (2009), [Erratum: Phys.Rev.D 82, 099902 (2010)], 0807.2722.
- [27] Y. Zhang, T. Zhong, H.-B. Fu, W. Cheng, and X.-G. Wu, Phys. Rev. D **103**, 114024 (2021), 2104.00180.
- [28] H. Hassanabadi, S. Rahmani, and S. Zarrinkamar, Eur. Phys. J. C **74**, 3104 (2014), 1407.3901.
- [29] N. Das and R. Dutta, J. Phys. G **47**, 115001 (2020), 1912.06811.
- [30] K. Azizi, R. Khosravi, and F. Falahati, Int. J. Mod. Phys. A **24**, 5845 (2009), 0811.2671.
- [31] R. N. Faustov and V. O. Galkin, Phys. Rev. D **87**, 034033 (2013), 1212.3167.

TABLE V: Fitted parameters $F(0)$, a_1 , and a_2 for V , A_0 , A_1 and A_2 in transition of $B_s \rightarrow D_s^*$.

	$F(0)$	a_1	a_2
$V^{dipole}(q^2)$	0.9764 ± 0.1520	1.4011 ± 0.6031	0.2931 ± 0.8256
$V^{exponential}(q^2)$	0.9817 ± 0.1534	0.0327 ± 0.0157	0.0007 ± 0.0003
$A_0^{dipole}(q^2)$	0.6195 ± 0.0495	2.0026 ± 0.3044	1.1041 ± 0.5948
$A_0^{exponential}(q^2)$	0.6146 ± 0.0551	0.0452 ± 0.0099	0.0005 ± 0.0003
$A_1^{dipole}(q^2)$	0.5905 ± 0.0404	1.1606 ± 0.3248	-0.0653 ± 0.7595
$A_1^{exponential}(q^2)$	0.5923 ± 0.0410	0.0241 ± 0.0082	0.0005 ± 0.0004
$A_2^{dipole}(q^2)$	0.5819 ± 0.0918	1.4000 ± 0.4201	0.0050 ± 0.0027
$A_2^{exponential}(q^2)$	0.5699 ± 0.1177	0.0355 ± 0.0229	0.0006 ± 0.0004

TABLE VI: Same as Table II for semileptonic transition of $B_s \rightarrow D_s^* \ell \nu_\ell$.

Mode	Γ with dipole	Γ with exponential	BR with dipole	BR with exponential
$B_s^0 \rightarrow D_s^{*-} \mu^+ \nu_\mu$	22.5097 ± 1.9921	22.5702 ± 1.9182	5.2246 ± 0.4624	5.2386 ± 0.4452
$B_s^0 \rightarrow D_s^{*-} e^+ \nu_e$	22.6055 ± 0.5942	22.6720 ± 0.6018	5.2468 ± 0.1379	5.2623 ± 0.1397
$B_s^0 \rightarrow D_s^{*-} \tau^+ \nu_\tau$	5.6349 ± 0.1549	5.6228 ± 0.1549	1.3079 ± 0.0359	1.3051 ± 0.0360

TABLE VIII: Same as Table IV for semileptonic transition of $B_s \rightarrow D_s^* \ell \nu_\ell$.

	$\langle P_L^e \rangle$	$\langle P_L^\mu \rangle$	$\langle P_L^\tau \rangle$	$\langle P_T^e \rangle$	$\langle P_T^\mu \rangle$	$\langle P_T^\tau \rangle$	$\langle C_F^e \rangle$	$\langle C_F^\mu \rangle$	$\langle C_F^\tau \rangle$
dipole	1.0000	0.9865	0.5198	-0.0002	-0.0432	-0.0499	-0.3712	-0.3582	-0.0496
exp	1.0000	0.9866	0.5201	-0.0002	-0.0432	-0.0491	-0.3744	-0.3611	-0.0486

TABLE VII: Forward-backward asymmetry and longitudinal polarization of vector meson for semileptonic transition of $B_s \rightarrow D_s^* \ell \nu_\ell$.

	$\langle \mathcal{A}_{FB}^e \rangle$	$\langle \mathcal{A}_{FB}^\mu \rangle$	$\langle \mathcal{A}_{FB}^\tau \rangle$	$\langle F_L^e \rangle$	$\langle F_L^\mu \rangle$	$\langle F_L^\tau \rangle$
dipole	-0.2700	-0.2743	-0.3295	0.4983	0.4981	0.4401
exponential	-0.2692	-0.2736	-0.3295	0.4997	0.4994	0.4391

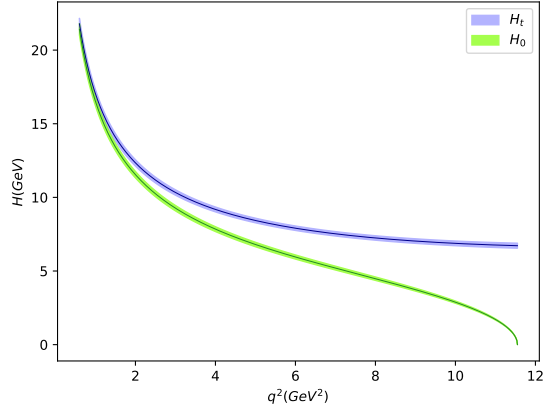


FIG. 9: The helicity amplitudes versus q^2 for $B_s \rightarrow D_s$ decay.

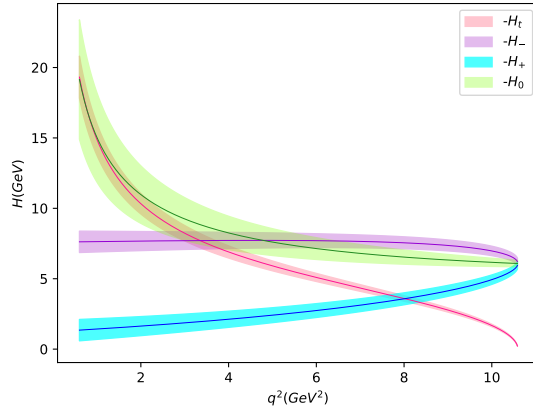


FIG. 10: The helicity amplitudes in the transition of $B_s \rightarrow D_s^*$ decay.

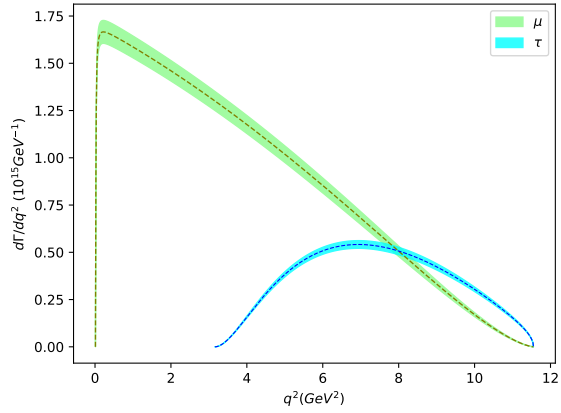


FIG. 11: The differential decay width for the semi-muonic and semi-tauonic channels of $B_s \rightarrow D_s$.

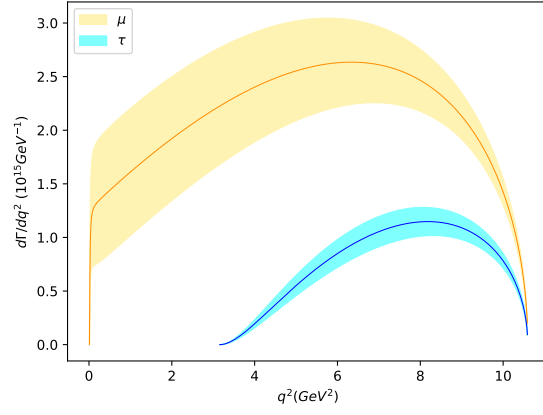


FIG. 12: Same as Fig. 11 for $B_s \rightarrow D_s^*$.

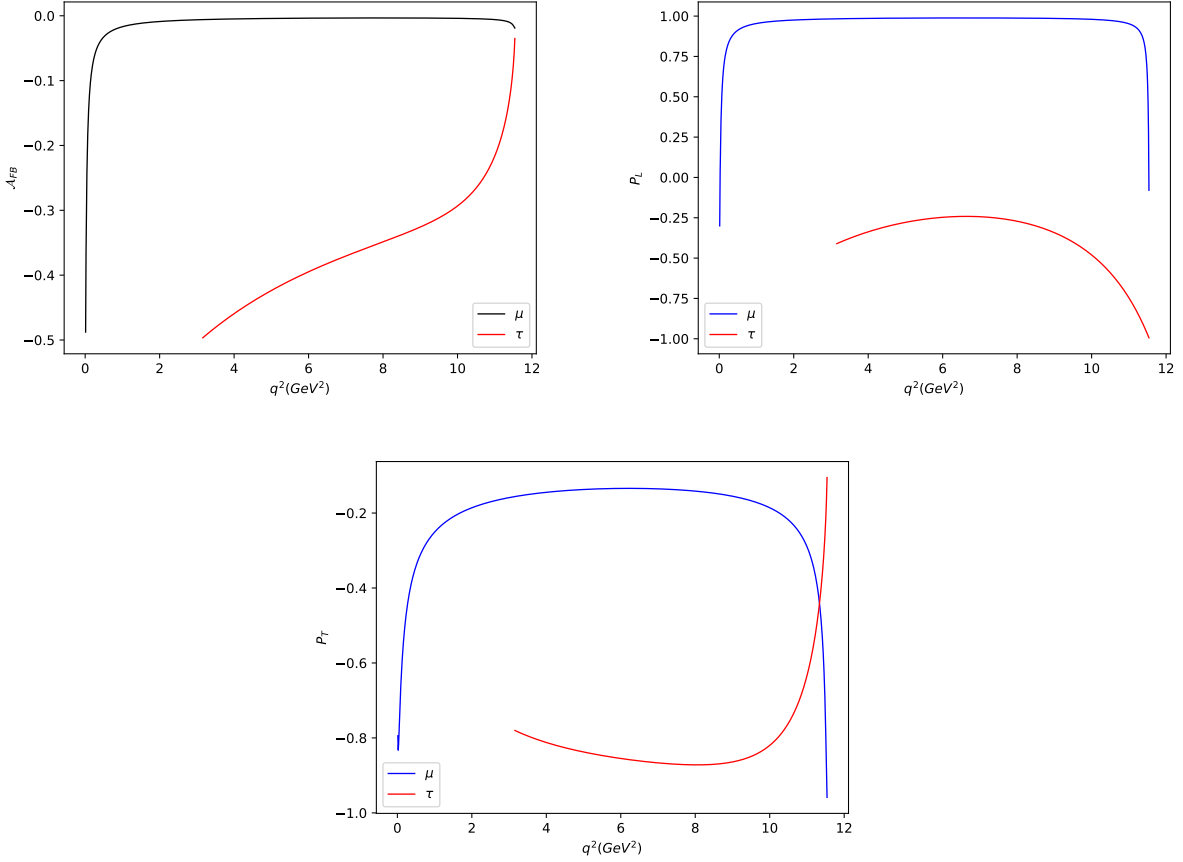


FIG. 13: The forward-backward asymmetries, longitudinal and transverse polarization of a charged lepton of the decays $B_s \rightarrow D_s \ell^+ \nu$.

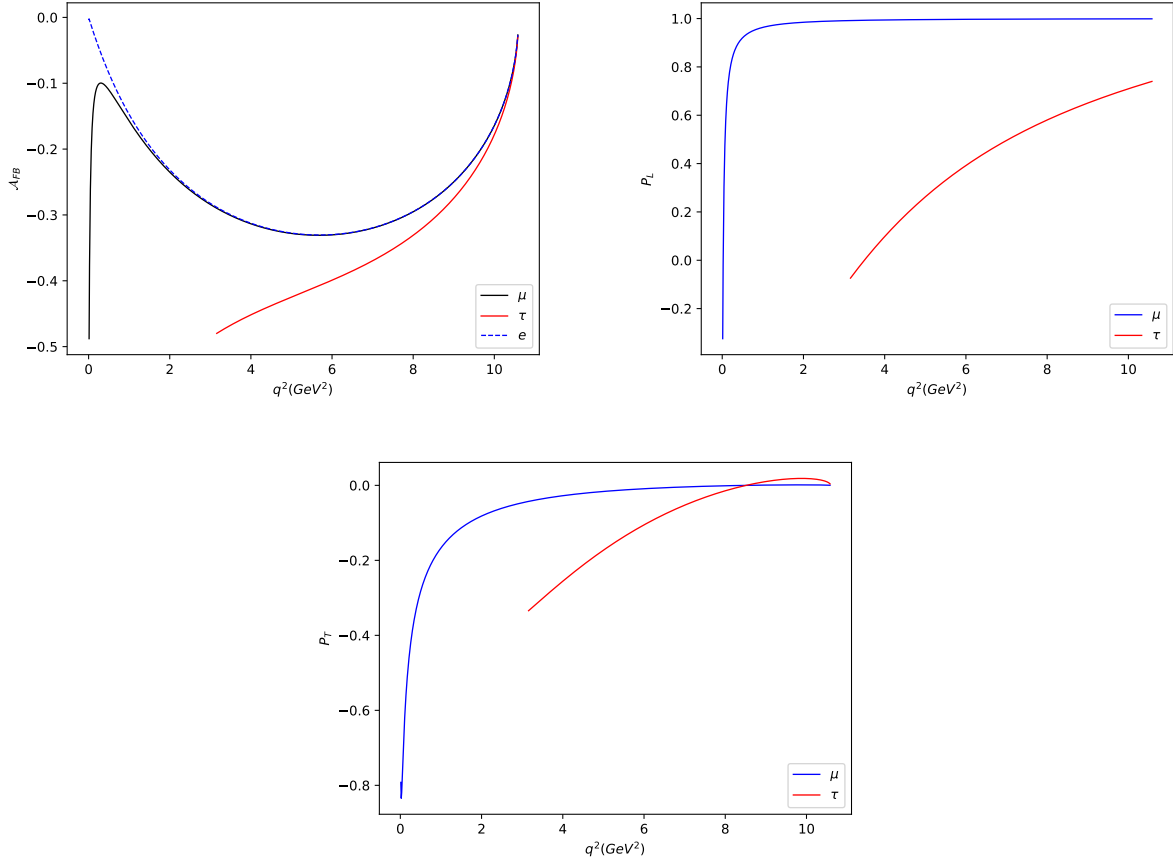


FIG. 14: Same as Fig. 13 for the decay $B_s \rightarrow D_s^* l \nu$

TABLE IX: Branching fractions for the indicated decay channels $B_s \rightarrow PP, B_s \rightarrow PV$ in percentage

Modes	Exponential	Dipole	PDG [25]	[30]	[31]	[8]
$B_s \rightarrow D_s^- \pi^+$	0.3197 ± 0.0118	0.3197 ± 0.0111	$(2.98 \pm 0.14) \times 10^{-1}$	-	0.35	0.53
$B_s \rightarrow D_s^- K^+$	0.0242 ± 0.0009	0.0242 ± 0.0008	$(2.25 \pm 0.12) \times 10^{-2}$	-	0.028	0.04
$B_s \rightarrow D_s^- D_s^+$	1.1221 ± 0.0341	1.1227 ± 0.0332	$(4.4 \pm 0.5) \times 10^{-1}$	-	1.1	-
$B_s \rightarrow D_s^- \rho^+$	0.0165 ± 0.0006	0.0165 ± 0.0006	$(6.8 \pm 1.4) \times 10^{-1}$	-	0.94	1.26
$B_s \rightarrow D_s^- D_s^{*+}$	0.1890 ± 0.0080	0.1889 ± 0.0079	-	$(2.62 \pm 0.93) \times 10^{-1}$	1.0	-